

The 1.1 Å Crystal Structure of Human TGF-β Type II Receptor Ligand Binding Domain

Christian C. Boesen,^{1,4} Sergei Radaev,^{1,4}
Shawn A. Motyka,² Apisit Patamawenu,¹
and Peter D. Sun^{1,3}

¹Structural Biology Section
Laboratory of Immunogenetics
National Institute of Allergy and Infectious Diseases
National Institutes of Health
Rockville, Maryland 20852

²Johns Hopkins University School of Medicine
Baltimore, Maryland 21205

Summary

Transforming growth factor β (TGF-β) is involved in a wide range of biological functions including development, carcinogenesis, and immune regulation. Here we report the 1.1 Å resolution crystal structure of human TGF-β type II receptor ectodomain (TBRII). The overall structure of TBRII is similar to that of activin type II receptor ectodomain (ActRII) and bone morphogenic protein receptor type IA (BRIA). It displays a three-finger toxin fold with fingers formed by the β strand pairs β1-β2, β3-β4, and β5-β6. The first finger in the TBRII is significantly longer than in ActRII and BRIA and folds tightly between the second finger and the C terminus. Surface charge distributions and hydrophobic patches predict potential TBRII binding sites.

Introduction

Transforming growth factor β (TGF-β) is found in most eukaryotic organisms including *C. elegans*, *Drosophila*, *Xenopus*, mice, and humans. It is expressed by virtually every cell type in most stages of development and is involved in a wide range of biological functions including development, epithelial cell growth, carcinogenesis, and immune regulation [1]. TGF-β is considered an essential component in the regulation of the immune system [2].

Structurally, TGF-β belongs to a superfamily of homologous growth factors that share at least 25% sequence identity in their mature amino acid sequence. There are 26 known mammalian TGF-β superfamily members and various other nonmammalian superfamily members. These include activin, bone morphogenic protein (BMP), growth and differentiation factor (GDF), nodal, dorsalin, Müllerian inhibiting substance (MIS), inhibin, and glial cell-derived neurotrophic factor (GDNF). Based on amino acid sequence homology and functional properties, the TGF-β superfamily receptors are divided into two branches, the type I and type II receptors. In mammals, there are seven known type I receptors and five known type II receptors. The type I receptors have a higher level of amino acid sequence homology to each other than do the type II receptors, especially within the kinase domain [1].

In vivo, TGF-β binds to the cell surface receptor TBRII,

forming a heterodimer capable of recruiting and activating the type I receptor (TBRI). In the absence of TBRII, TGF-β has no affinity for TBRI. Activin and MIS also use this sequential mode of binding. BMP-2, BMP-7, GDF-5, and Dpp, however, use a cooperative mode of binding. In this second binding mode, the ligand has a low affinity for both the type I and type II receptors when expressed separately, but a high affinity when expressed together. Upon complex formation, the constitutively active serine/threonine kinase in the cytoplasmic domain of TBRII phosphorylates the kinase domain of TBRI, thereby initiating a signaling cascade through the SMAD molecules [1, 3].

TGF-β exists in five different isoforms that share 66%–80% sequence identity. Forms 1–3 are found in human, while forms 4 and 5 are found in chicken and *Xenopus*, respectively. The growth factor is expressed with an N-terminal latent peptide that is cleaved to release the 112 residue mature TGF-β. X-ray structure determination has demonstrated that TGF-β forms a disulfide-bonded homodimer having a cysteine-knot structure [4–8].

TBRII is a type I transmembrane glycoprotein containing a 136 residue TGF-β binding domain, a single transmembrane region, and an intracellular kinase domain [9]. The TGF-β binding domain contains 12 cysteine residues. The structure of the murine ActRII extracellular domain [10] and a complex between human BMP-2 and its type I receptor extracellular domain [11] show that both receptors have a three-finger toxin fold, similar to some snake venom neurotoxins.

Here we report the structure of TBRII ectodomain at 1.1 Å resolution. The analysis of TBRII structure and its comparison to previously determined structures of ActRII and BRIA allow us to make predictions about probable folding of other members of the TGF-β receptor superfamily. In addition, surface charge distributions and hydrophobic patches predict potential TBRII binding sites.

Results and Discussion

Structure Solution

The crystals belong to space group P2₁2₁2₁, with cell dimensions $a = 35.5$, $b = 40.7$, and $c = 76.2$ Å, with one monomer of TBRII in each asymmetric unit. The structure of the TBRII ectodomain was solved by the multiwavelength anomalous dispersion (MAD) method using an HgCl₂ derivative crystal. The electron density map calculated from the MAD phases was of good quality and automatically traced by the ARP/wARP program (Figure 1) [12]. The structure was refined to 1.1 Å resolution with a final R_{cryst} of 15.6% ($R_{\text{free}} = 16.6\%$; Table 1). The refined model contains TBRII residues 26–131, a well-defined glycerol molecule, and 176 water molecules. TBRII C-terminal residues 132–136 were disordered.

³Correspondence: psun@nih.gov

⁴These two authors contributed equally to this work.

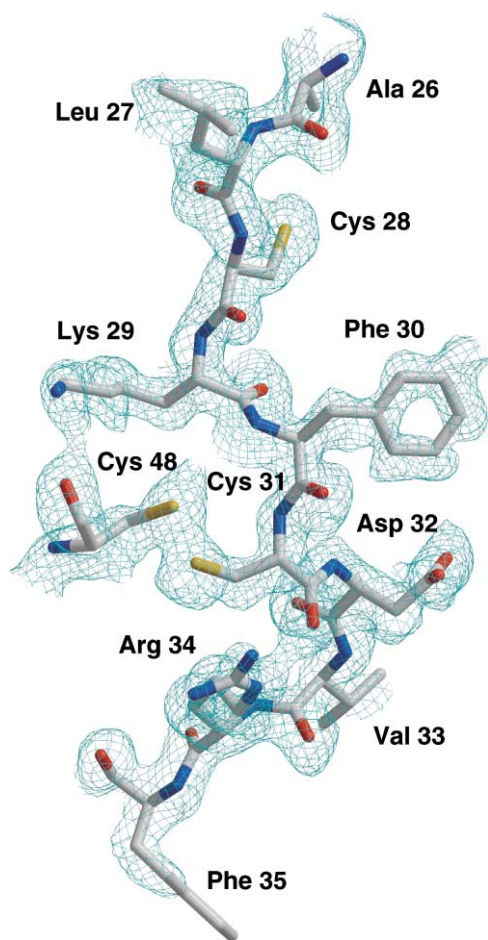


Figure 1. Representative Section of Experimental Electron Density. The map is calculated with solvent-flattened MAD phases, contoured at 1.0 σ level. The refined atomic model of the TBR11 ectodomain is shown in stick representation.

General Architecture

The overall structure of the TBR11 ectodomain consists of two antiparallel β sheets. Strands $\beta 2$, $\beta 1$, $\beta 4$, $\beta 3$, $\beta 6$, and $\beta 5$ form the larger sheet, while strands $\beta 1'$, $\beta 1''$, and $\beta 7$ form the smaller sheet (Figure 2). The TBR11 structure has a three-finger toxin fold similar to some snake venom neurotoxins, which is characteristic for proteins having a common pattern of eight cysteines forming four disulfide bonds. The first finger contains a bend with the first portion formed by strands $\beta 1$ and $\beta 2$, and the second by strands $\beta 1'$ and $\beta 1''$. Strands $\beta 3$ and $\beta 4$ form the second finger, while strands $\beta 5$ and $\beta 6$ form the third finger.

TBR11 contains four disulfide bonds conserved among the type II TGF- β receptor superfamily and two disulfide bonds unique to TBR11 (Figure 3). The conserved disulfide bonds include Cys 28-Cys 61 between the $\beta 1$ and $\beta 3$ strands, Cys 54-Cys 78 between the $\beta 2$ and $\beta 4$ strands, Cys 98-Cys 113 between the $\beta 5$ and $\beta 6$ strands, and Cys 115-Cys 120 between the $\beta 6$ strand and the loop between the $\beta 6$ and $\beta 7$ strands. The disulfide bonds Cys 31-Cys 48 between the $\beta 1$ strand and the loop between the $\beta 1'$ and $\beta 2$ strands, and Cys 38-Cys 44

between the $\beta 1'$ and $\beta 1''$ strands exist exclusively in TBR11.

Structural Homologs

The structure of TBR11 and the previously published structures of ActR11 and BR1A could be superimposed onto each other with root-mean-square deviations of 1.6 Å between TBR11 and ActR11 (62 C α atoms), 2.4 Å between TBR11 and BR1A (40 C α atoms), and 2.5 Å between ActR11 and BR1A (54 C α atoms) (Figure 4). The three longest β strands, $\beta 3$, $\beta 4$, and $\beta 6$, which are part of the larger β sheet, overlay well among all three structures (Figure 4). The most striking difference between the TBR11 and both the ActR11 and BR1A structures is located in their first finger. Finger one in the TBR11 structure is significantly longer than the corresponding counterparts in the ActR11 and BR1A structures. It contains 18 residues (Asp 32-Ser 49), whereas the same region has 11 (Asn 15-Gln 25), and 10 (Gly 42-Asn 51) residues in ActR11 and BMP, respectively. Structurally, the bottom of the first finger, the $\beta 1$ and $\beta 2$ strands, lies in a similar position for all three structures. The difference occurs at the top of the first finger, where TBR11 contains two antiparallel β strands ($\beta 1'$ and $\beta 1''$) linked together by two unique disulfide bonds Cys 31-Cys 48 and Cys 38-Cys 44. In this position, ActR11 contains an α helix which points in the direction opposite to that of the $\beta 1'/\beta 1''$ strands of TBR11 (Figure 4A). The distance between the tips of the first fingers in the TBR11 and ActR11 structures is about 30 Å. The top part of finger one in BR1A is formed by a loop that bends even further down compared to the similar part of the ActR11 structure (Figure 4C). The spatial difference between ActR11 and BR1A in this part of the structure is 11 Å. Moreover, the BR1A structure contains a disulfide bond, which is characteristic for all type I, but is not found in type II, receptors (Figure 3). The structure of the BMP-2/BR1A complex revealed that finger one of BR1A is involved in the binding of its ligand BMP-2. Therefore, it is plausible to suggest that the role of this disulfide bond in finger one of type I receptors is to restrict the flexibility of the top part of the finger and to bring it into the optimal position for ligand binding.

The $\beta 1'$ and $\beta 1''$ strands of TBR11 contact the upper portion of finger two ($\beta 3$ and $\beta 4$ strands). All three receptors overlay well in finger two. The only significant difference occurs in the upper portion of finger two, which is noticeable when TBR11 and ActR11 structures are superimposed (Figure 4A). The upper portion of finger two is flatter in TBR11 compared to the inward bending ActR11. This results in the corresponding loops of finger two in TBR11 and ActR11 being separated by 10 Å. The same loop is disordered in the structure of BR1A/BMP-2 complex.

Two longer antiparallel β strands $\beta 5$ and $\beta 6$ form the third finger in the structure of TBR11. They run closer to each other compared to the structure of ActR11, where the corresponding strands are shorter and more diverged. The structure of BR1A lacks the $\beta 5$ strand completely. Instead, it has a long loop that connects the short $\alpha 3$ helix to the $\beta 6$ strand. Another unique feature of TBR11 is the absence of a conserved disulfide bond observed in other type I and type II receptors. This con-

Table 1. Data Collection, Phasing, and Refinement Statistics

	Native	Hg (remote)	Hg (peak)	Hg (edge)
Data Collection				
Wavelength (Å)	1.0092	1.0011	1.0076	1.0092
Resolution limit (Å)	1.05	1.44	1.30	1.34
Unique reflections	45,991 (2,277) ^a	33,021 (2,975)	47,303 (3,472)	41,063 (3,461)
Redundancy	8.5 (3.9)	2.2 (2.2)	2.4 (1.5)	2.2 (1.7)
Completeness (%)	87.9 (44.3)	87.6 (79.5)	92.1 (67.6)	87.5 (73.1)
R _{sym} (%) ^b	3.5 (48.8)	3.8 (35.7)	2.9 (24.3)	3.0 (31.3)
$\langle I/\sigma(I) \rangle$	56.5 (2.8)	19.4 (1.8)	27.6 (2.7)	26.6 (2.2)
Phasing (36–1.4 Å)				
Mean figure of merit			0.62	
R _{Cullis} ^c		0.69	0.44	0.48
Phasing power ^d		1.48	3.70	3.47
Refinement				
Resolution (Å)	36–1.05			
Number of reflections	43,635			
Number of protein atoms	828			
Number of solvent atoms	184			
R _{cryst} (%)	15.6 (29.2)			
R _{free} (%) ^e	16.6 (29.0)			
Mean B factor (Å ²)	12			
Wilson B factor (Å ²)	8.0			
Rmsd bond lengths (Å)	0.007			
Rmsd bond angles (°)	1.48			
Ramachandran statistics ^f	88.7%	11.3%	0.0%	0.0%

^a Values for highest resolution shells 1.09–1.05 (native), 1.49–1.44 (remote), 1.35–1.30 (peak), and 1.39–1.34 (edge) Å are given in brackets.

^b $R_{sym} = 100 \times \sum |I_h - \langle I_h \rangle| / \sum I_h$, where $\langle I_h \rangle$ is the mean intensity of multiple measurements of symmetry equivalent reflections.

^c $R_{Cullis} = \text{rms}(E) / \text{rms}(\Delta F)$, where E is the phase-integrated lack of closure and ΔF is the dispersive or anomalous difference.

^d Phasing power = $\text{rms}(F_H) / \text{rms}(E)$, where F_H is the calculated heavy atom structure factor.

^e R_{free} was calculated using test set of 5%.

^f Percentages of residues are shown for the most favored region, additional allowed region, generously allowed region, and disallowed region of the Ramachandran plot.

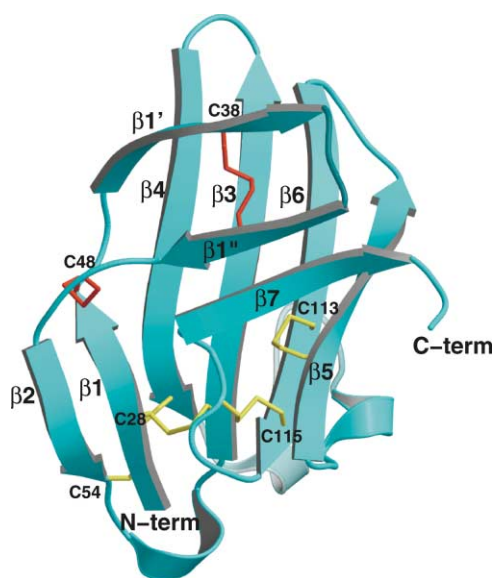


Figure 2. Ribbon Drawing of the TBR II Ectodomain

All β strands are marked in accordance with the sequence alignment in Figure 3. The disulfide bonds common to TBR II and ActR II are in yellow (C28–C61, C54–C78, C98–C113, and C115–C120). The disulfide bonds unique to TBR II are in red (C31–C48 and C38–C44). This figure and the subsequent ribbon drawings were prepared using the programs MOLSCRIPT [26] and Raster3D [27].

served disulfide is located between the $\alpha 3$ helix and the $\beta 6$ strand (Cys 66–Cys 85 in ActR II and Cys 87–Cys 101 in BR I A). At this conserved disulfide location, TBR II has a hydrogen bond between Asp 92 and Ser 114 (Figures 4A and 4B). In contrast, BR I A, like other mammalian type I receptors, lacks the Cys 98–Cys 113 disulfide bond (TBR II numbering) that connects the $\beta 5$ and $\beta 6$ strands in type II structures (Figure 4B).

Sequence Homologs

There are common features in the pattern of disulfide bonds among members of the mammalian TGF- β superfamily type I and type II receptors (Figure 3). These include three structurally identical disulfide bonds Cys 28–Cys 61, Cys 54–Cys 78, and Cys 115–Cys 120 (TBR II numbering) that are conserved among all mammalian type I and type II receptors. TBR II lacks a fourth disulfide bond between the $\alpha 3$ and the $\beta 6$ strand that is conserved among all other mammalian receptors. Here, instead of the cysteines observed in other sequences, TBR II has Asp 92 and Ser 114 in the corresponding positions. These residues form a hydrogen bond of 2.7 Å between the O $\delta 1$ atom of Asp 92 and the O γ atom of Ser 114. Compared to mammalian type I receptors, all mammalian type II receptors have an additional disulfide bond Cys 98–Cys 113 that connects the $\beta 5$ and $\beta 6$ strands.

In addition to these conserved disulfide bonds, there are distinct differences in receptor disulfide bond architecture. TBR II has two unique disulfide bonds, Cys 31–Cys 48 and Cys 38–Cys 44, located in finger one that bridge together opposite sides of the upper portion of

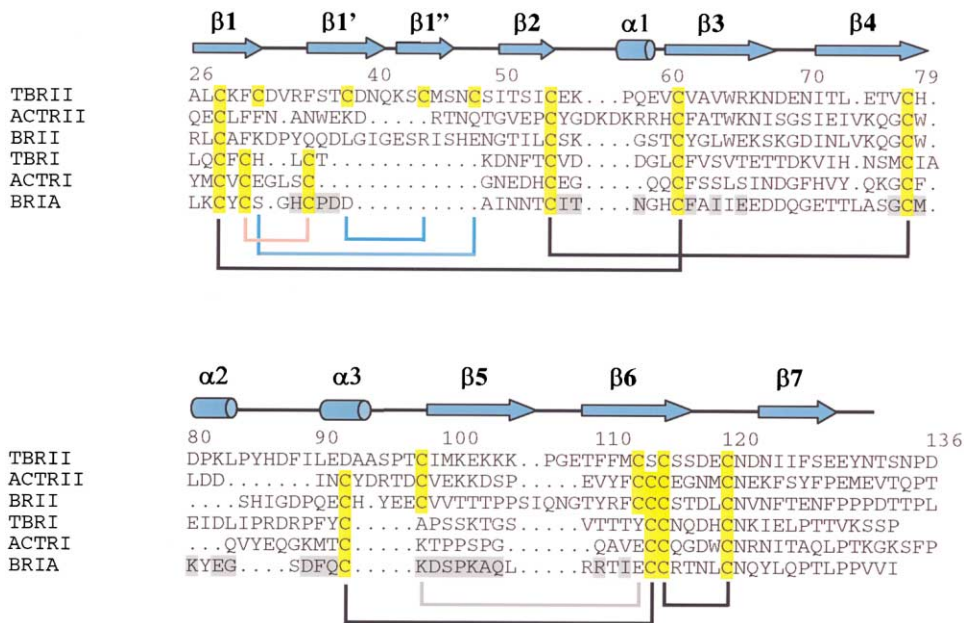


Figure 3. The Amino Acid Sequences of TGF- β , Activin, and BMP Receptor Type I and II Ectodomains

Gaps are indicated with (.). The numbering is consistent with the mature sequence of TBRII except for the engineered mutations T26A and K97T. The secondary structure elements of TBRII are illustrated as arrows for β strands and as cylinders for α helices. These elements correspond to the following TBRII residues: β 1 (26–31), β 1' (34–40), β 1'' (42–46), β 2 (50–54), β 3 (60–68), β 4 (71–79), β 5 (96–104), β 6 (108–116), β 7 (122–127), α 1 (56–59), α 2 (80–83), and α 3 (90–93). The BRIA residues involved in ligand-receptor interactions are highlighted in gray. The cysteine residues are highlighted in yellow. Disulfide bridges that are common among all mammalian receptors are given in black, one unique to mammalian type II receptors in gray, two unique to TBRII in cyan, and one characteristic of mammalian type I receptors in pink. All sequences are human except for ActRII (mouse).

the finger (Figures 2 and 4). Mammalian type I receptors have a conserved disulfide bond, Cys 40-Cys 44 (BRIA numbering), which is also located in finger one. However, the placement and architecture of this disulfide bond is different from that of TBRII, Cys 31-Cys 48.

Instead of bridging opposite sides of finger one (like in TBRII), this disulfide bond connects cysteine residues that are only 3 residues apart in the BRIA structure and located on the same side of the finger. As it was pointed out above, a possible function of this disulfide bond,

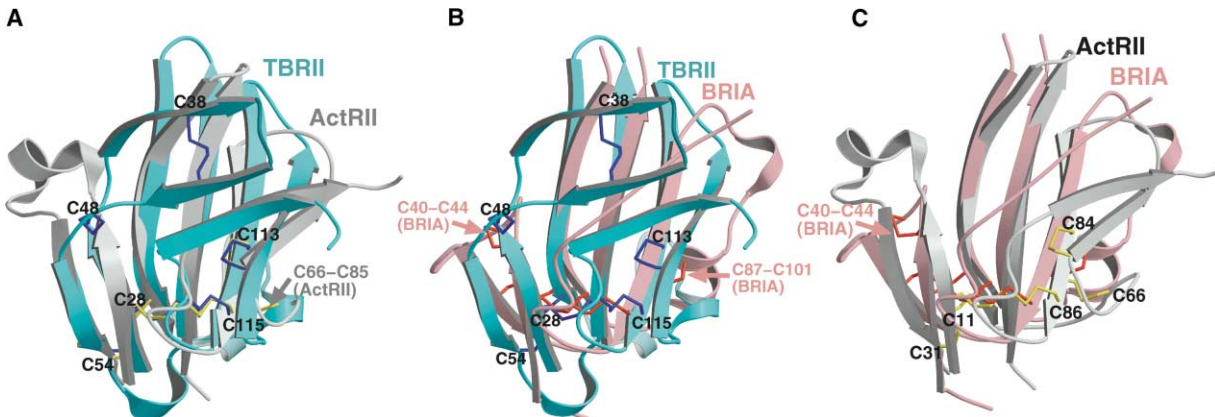


Figure 4. Structural Comparison of Ectodomains of Some Members of the TGF- β Superfamily

(A) Structural comparison between TBRII (cyan) and ActRII (gray) ectodomains. The numbering is consistent with the mature sequence of TBRII. Disulfide bridges of TBRII (C28-C61, C31-C48, C54-C78, C98-C113, and C115-C120) are blue. Disulfide bridges of ActRII (C11-C41, C31-C59, C66-C85, C72-C84, and C86-C91) are yellow. The coordinates for the ActRII ectodomain are taken from Protein Data Bank entry 1bte.

(B) Structural comparison between TBRII (cyan) and BRIA (pink) ectodomains. The numbering is consistent with the mature sequence of TBRII. Disulfide bridges of TBRII are blue. Disulfide bridges of BRIA (C38-C59, C40-C44, C55-C77, C87-C101, and C102-C107) are red. The coordinates for the BRIA ectodomain are taken from Protein Data Bank entry 1es7.

(C) Structural comparison between ActRII (gray) and BRIA (pink) ectodomains. The numbering is consistent with the mature sequence of ActRII. Disulfide bridges of ActRII are yellow and of BRIA are red.

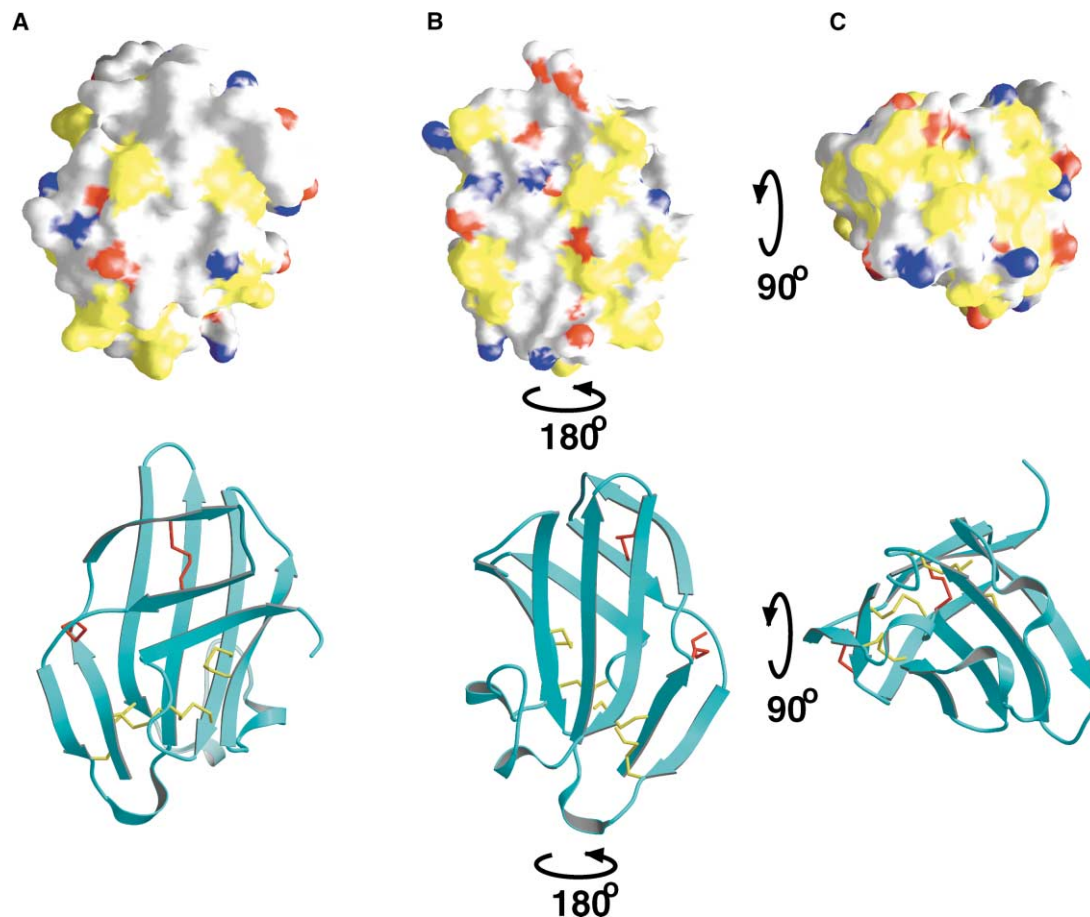


Figure 5. Surface Representation of Charge Distribution and Hydrophobic Patches on TBRII

(A) Orientation of the molecule corresponds to that of Figures 2 and 4.

(B) Molecule is rotated about 180 degrees around the vertical axis compared to (A).

(C) Molecule is rotated about 90 degrees around the horizontal axis compared to (A). Ribbon drawings in the lower panel are given as an orientation reference. Hydrophobic patches are colored yellow. Positive and negative charges are colored blue and red, respectively.

which is conserved among the mammalian type I receptors, could be to restrict the movement of finger one and bring it into the optimal position for ligand binding.

An examination of the type I and type II receptor amino acid sequences from three members of the mammalian TGF- β superfamily provides predictive information about the structures of BRII, TBRI, and ActRI (Figure 3). The length of the first finger region in the BRII sequence is exactly the same as in the TBRII sequence, suggesting that BRII will have a secondary structure similar to the $\beta 1' / \beta 1''$ antiparallel β strands of finger one in TBRII. The absence of TBRII finger one disulfide bonds (Cys 31-Cys 48 and Cys 38-Cys 44; TBRII numbering) in BRII might be compensated for by salt bridges/hydrogen bonds between Lys 31 and Glu 48 and between Asp 37 and Arg 44 residues (TBRII numbering; Figure 3) located around respective TBRII cysteines in the sequence alignment (Figure 3).

This same finger one region is significantly (11–14 residues) shorter than the corresponding region of TBRII and BRII for all mammalian type I receptors. In addition, mammalian type I receptors have a conserved disulfide bond, Cys 40-Cys 44 (BRIA numbering), that may restrict

the flexibility of the loop on the tip of finger one and bring this loop into the optimal position for ligand binding. This suggests that other mammalian type I receptors will have a finger one similar to BRIA in overall shape and position.

The absence of the Cys 98-Cys 113 disulfide bond (TBRII numbering) in BRIA may be linked to the absence of the $\beta 5$ strand in the structure of BRIA. Therefore, other mammalian type I receptor structures might have the same long loop running parallel to the $\beta 6$ strand and connecting the short helix $\alpha 3$ to the $\beta 6$ strand.

In summary, the results of structure analysis and sequence alignment suggest that the overall fold of the BRII structure will be similar to TBRII, with two antiparallel β strands in the upper part of finger one forming a core of the second short antiparallel β sheet. The TBRI and ActRI structures would be predicted to be similar to their type I receptor counterpart, BRIA.

Putative Binding Sites of TBRII

Upon cell surface activation, TGF- β forms a ternary complex with both type I and type II receptors. The type II receptor, owing to its nanomolar affinity to TGF- $\beta 1$ (data

not shown), presumably serves as the primary recruiting receptor for the ligand. The type I receptor, in contrast, lacks appreciable affinity to TGF- β in the absence of the type II receptor and is likely recruited to the TBR1I/TGF- β heterodimeric complex to form the final trimeric complex. The unique role of TBR1I in bridging the ternary complex formation suggests two binding surfaces, one with TGF- β and another with TBR1. Based on the current TBR1I structure and the available structures of ActR1I and BR1A/BMP-2 complex, the putative ligand and type I receptor binding regions are proposed here.

Structural analysis of BR1A/BMP-2 complex [11] revealed predominantly hydrophobic interactions at the binding interface. Previous studies have shown that large surface-exposed hydrophobic patches often constitute binding surfaces [13], as seen in the human growth hormone-growth hormone receptor complex [14]. Analysis of the charged versus hydrophobic residue distribution on the TBR1I surface reveals three extensive hydrophobic patches that could be candidate TGF- β and TBR1 binding sites (Figure 5). The largest surface patch, approximately 700 Å² in size, is located on the "bottom" of TBR1I (in the area of conserved disulfide bonds). It contains the N termini of the β 1, β 3, and β 5 strands, the C termini of the β 2, β 4, and β 6 strands, as well as the α 1, α 2, and α 3 helices (Figure 5C). As TBR1I possesses higher binding affinity for TGF- β than for TBR1, it is tempting to speculate that this largest surface patch corresponds to the binding site for TGF- β . This region contains a unique disulfide bond on the first finger and the presence of the β 5 strand, constituting the major structural differences between the type I and type II receptors, which may reflect their differences in ligand binding (Figures 3 and 4). The involvement of this surface patch in TGF- β binding is supported by the binding studies of TBR1I deletion mutants [15]. It was found through a series of TBR1I deletion mutants that only the following mutants disrupt the binding of TGF- β 1 to the receptor: Δ F35-T37, Δ N40-K42, and Δ M45-N47, which are located in the first finger, and Δ E55-P57, Δ D80-K82, and Δ S95-T97, which are in the largest hydrophobic patch. The next prominent hydrophobic patch, a possible site for TBR1 binding, is about 500 Å² in size and is located on the "back side" of the molecule (Figure 5B). It includes the β 2 and β 4 strands, a tip of the α 2 helix, and a loop connecting the α 2 and α 3 helices. Interestingly, this region is also topologically equivalent to the BMP-2 binding site on BR1A. The third patch is in the "front" of the molecule. It is the smallest patch (about 250 Å²) among the three and is also more fragmented than the previous two patches (Figure 5A). It comprises the N terminus of the β 1' strand, the C terminus of the β 7 strand, and a small portion of the β 5 strand. In addition, the location of the third patch is consistent with it being orientated toward the plasma membrane, thus making it unlikely to be involved in either TGF- β or type I receptor binding.

The structure of ActR1I revealed a conserved hydrophobic patch located near the central part of the structure [10]. This hydrophobic patch in ActR1I consists of Phe 42 and Trp 45 from its β 3 strand, Ile 52 and Ile 54 from the β 4 strand, Tyr 82 from the β 6 strand, and Tyr 87 and Phe 95 from the β 7 strand. Mutations of

ActR1I in this region, including F42A, W60A, and F83A, have been produced and result in a loss in receptor binding to activin and inhibin [16]. The same region of TBR1I, however, is completely covered by its long first finger and is no longer surface exposed. This difference between TBR1I and ActR1I may contribute to their unique ligand recognition.

Biological Implications

In general, TGF- β inhibits cell growth, and mutations in the TBR1I are associated with cancer. Most sporadic colon and gastric cancers have an inactive TBR1I, and mutations in the receptor have also been identified in T cell lymphoma, and head and neck carcinomas [1]. Given the wide range of biological functions, design of blocking agents that distinguish between various TGF- β receptors could have important pharmacological implications. Structural differences between different members of the TGF- β receptor superfamily will aid in the design of potential therapeutic agents. The striking difference in the structure of TBR1I compared to ActR1I and BR1A is structure and location of the β 1'/ β 1" strand at the top of finger one. Sequence homology suggests that this structural feature will be more typical of most type II receptors rather than the α helix in finger one of the ActR1I structure. This information could be potentially useful in designing agents that specifically block interactions between type II receptors and their ligands or between type II and type I receptors.

Experimental Procedures

Sample Preparation and Crystallization

Human TBR1I (T26A/K97T) residues 26–136 was expressed in *E. coli* as inclusion bodies and refolded as previously described [17]. Crystallization was carried out using the vapor diffusion method with drops containing TBR1I ectodomain (20 mg ml⁻¹) and 30% PEG 2000 with 0.1 M Na citrate (pH 5.0) as described in details elsewhere [18].

Data Collection and Structure Determination

After a brief soaking in precipitant solutions containing 25% glycerol, crystals were flash frozen at 100 K. X-ray diffraction data from single crystals were collected using an ADSC Quantum IV CCD detector at the X9B beamline of the National Synchrotron Light Source (NSLS), Brookhaven National Laboratory and processed with HKL2000 [19]. A MAD data set was collected from crystals soaked in HgCl₂ at the X9B beamline (NSLS). Three Hg sites were found by SOLVE [20]. After density modification, including solvent flattening, the electron density was traced using the ARP/wARP autotracing program [12]. Model adjustments and rebuilding were done using the program O [21]. The initial positional and individual B factor refinement was carried out using a maximum likelihood target function of CNS v1.0 [22]. The final anisotropic refinement with maximum likelihood target function was carried out by REFMAC5 [23] from the CCP4 program suite [24].

Acknowledgments

We wish to thank A. Johnson, M. Kattah, and Z. Dauter for their assistance in synchrotron data collection.

Received: January 18, 2002

Revised: April 10, 2002

Accepted: April 19, 2002

References

1. Massague, J. (1998). TGF- β signal transduction. *Annu. Rev. Biochem.* 67, 753–791.
2. Letterio, J.J., and Roberts, A.B. (1998). Regulation of immune responses by TGF- β . *Annu. Rev. Immunol.* 16, 137–161.
3. Heldin, C.-H., Miyazono, K., and ten Dijke, P. (1997). TGF- β signaling from cell membrane to nucleus through SMAD proteins. *Nature* 390, 465–471.
4. Sun, D., Piez, K.A., Ogawa, Y., and Davies, D.R. (1992). Crystal structure of transforming growth factor- β 2: an unusual fold for the superfamily. *Science* 257, 369–373.
5. Schlunegger, M.P., and Grutter, M.G. (1992). An unusual feature revealed by the crystal structure at 2.2 angstrom resolution of human transforming growth factor- β 2. *Nature* 358, 430–434.
6. Sun, P.D., and Davies, D.R. (1995). The cysteine-knot growth-factor superfamily. *Annu. Rev. Biophys. Biomol. Struct.* 24, 269–291.
7. Hinck, A.P., Archer, S.J., Qian, S.W., Roberts, A.B., Sporn, M.B., Weatherbee, J.A., Tsang, M.L., Lucas, R., Zhang, B.L., Wenker, J., and Torchia, D.A. (1996). Transforming growth factor β 1: three-dimensional structure in solution and comparison with X-ray structure of transforming growth factor β 2. *Biochemistry* 35, 8517–8534.
8. Mittl, P.R.E., Priestle, J.P., Cox, D.A., McMaster, G., Cerletti, N., and Grutter, M.G. (1996). The crystal structure of TGF- β 3 and comparison to TGF- β 2: implications for receptor binding. *Protein Sci.* 5, 1261–1271.
9. Lin, H.Y., Wang, X.-F., Ng-Eaton, E., Weinberg, R.A., and Lodish, H.F. (1992). Expression cloning of the TGF- β type II receptor, a functional transmembrane serine/threonine kinase. *Cell* 68, 775–785.
10. Greenwald, J., Fischer, W.H., Vale, W.W., and Choe, S. (1999). Three-finger toxin fold for the extracellular TGF- β -binding domain of the type II activin receptor serine kinase. *Nat. Struct. Biol.* 6, 18–22.
11. Kirsch, T., Sebald, W., and Dreyer, M.K. (2000). Crystal structure of the BMP-2-BRIA ectodomain complex. *Nat. Struct. Biol.* 7, 492–496.
12. Perrakis, A., Morris, R., and Lamzin, V.S. (1999). Automated protein model building combined with iterative structure refinement. *Nat. Struct. Biol.* 6, 458–463.
13. Young, L., Jernigan, R.L., and Covell, D.G. (1994). A role for surface hydrophobicity in protein-protein recognition. *Protein Sci.* 3, 717–729.
14. Clackson, T., and Wells, J.A. (1995). A hot spot of binding energy in a hormone-receptor interface. *Science* 267, 383–386.
15. Guimond, A., Sulea, T., Pepin, M.-C., and O'Connor-McCourt, M.D. (1999). Mapping of putative binding sites on the ectodomain of the type II TGF- β receptor by scanning-deletion mutagenesis and knowledge-based modeling. *FEBS Lett.* 456, 79–84.
16. Gray, P., Greenwald, J., Blount, A.L., Kunitake, K.S., Donaldson, C.J., Choe, S., and Vale, W. (2000). Identification of a binding site on the type II activin receptor for activin and inhibin. *J. Biol. Chem.* 275, 3206–3212.
17. Boesen, C.C., Motyka, S.A., Patamawenu, A., and Sun, P.D. (2000). Development of a recombinant bacterial expression system for the active form of a human transforming growth factor β type II receptor ligand binding domain. *Protein Expr. Purif.* 20, 98–104.
18. Boesen, C.C., Motyka, S.A., Patamawenu, A., and Sun, P.D. (2002). Crystallization and preliminary crystallographic studies of human TGF- β type II receptor ligand binding domain. *Acta Crystallogr. D* 58, in press.
19. Otwinowski, Z., and Minor, W. (1997). Processing of X-ray diffraction data collected in oscillation mode. *Methods Enzymol.* 276, 307–326.
20. Terwilliger, T.C., and Berendzen, J. (1999). Automated MAD and MIR structure solution. *Acta Crystallogr. D* 55, 849–861.
21. Kleywegt, G.J., and Jones, T.A. (1996). Efficient rebuilding of protein structures. *Acta Crystallogr. D Biol. Crystallogr.* 52, 829–832.
22. Brunger, A.T., Adams, P.D., Clore, G.M., DeLano, W.L., Gros, P., Grosse-Kunstleve, R.W., Jiang, J.S., Kuszewski, J., Nilges, M., Pannu, N.S., et al. (1998). Crystallography & NMR system: a new software suite for macromolecular structure determination. *Acta Crystallogr. D Biol. Crystallogr.* 54, 905–921.
23. Murshudov, G.N., Lebedev, A., Vagin, A.A., Wilson, K.S., and Dodson, E.J. (1999). Efficient anisotropic refinement of macromolecular structures using FFT. *Acta Crystallogr. D* 55, 247–255.
24. CCP4 (Collaborative Computational Project 4) (1994). The CCP4 suite: programs for protein crystallography. *Acta Crystallogr. D* 50, 760–763.
25. Hart, P.J., Deep, S., Taylor, A.B., Shu, Z., Hinck, C.S., and Hinck, A.P. (2002). Crystal structure of the human T β R2 ectodomain-TGF- β 3 complex. *Nat. Struct. Biol.* 9, 203–208.
26. Kraulis, P. (1991). MOLSCRIPT: a program to produce both detailed and schematic plots of protein structures. *J. Appl. Crystallogr.* 24, 946–950.
27. Merritt, E.A., and Bacon, D.J. (1997). Raster3D: photorealistic molecular graphics. *Methods Enzymol.* 227, 505–524.

Note Added in Proof

While this manuscript was being revised, the structure of a human TBRII/TGF- β was published, confirming the largest surface patch on TBRII as being the ligand binding site [25].